Evaluation of LoRa Receiver Performance under Co-technology Interference

Guibing Zhu, Chun-Hao Liao, Makoto Suzuki, Yoshiaki Narusue and Hiroyuki Morikawa
Graduate School of Engineering, The University of Tokyo
7–3–1, Hongo, Bunkyo-ku, Tokyo, 113–8654 Japan
shukeihei@mlab.t.u-tokyo.ac.jp

***Abstract*—LoRa networks achieve a remarkably wide coverage as compared to that of the conventional wireless systems by employing the chirp spread spectrum (CSS). However, single-hop LoRa networks have limited penetration in indoor environments and cannot efficiently utilize the multiple-access dimensions arising from different spreading factors (SF) because the star topology is typically used for LoRa. On the other hand, a multi-hop LoRa network has the potential to realize extensive network coverage by utilizing packet relaying and improving the network capacity by utilizing different SFs. We evaluated the LoRa receiver performance under co-technology interference via simulation and experiments to realize these potentials.. The results show that LoRa can survive interference from time-synchronized packets transmitted by multiple transmitters with an identical SF. Furthermore, we examined the orthogonality between different SFs by evaluating the required signal-to-interference ratio (SIR). Finally, we demonstrated the possibility of employing different SFs to construct the pipeline in a multi-hop relay network to increase network efficiency.**

I. Introduction

In recent years, the LoRa, low-power wide-area network (LPWAN) specification, has attracted great attention. The merits of LoRa include not only wide coverage (with reported communication ranges of up to 15 km [1]) but also great flexibility to trade sensitivity for higher throughput (100 speedup by sacrificing 20dB sensitivity). In both academia and industry, many groups are dedicated towards the development of various LoRa applications, such as remote health and well-being monitoring systems [2], long-range surveillance systems [3], and object tracking and managing systems [4]. It has great potential for applications in domains like smart grid and smart agriculture. Till 2017, LoRa networks were widely deployed in over 50 countries [5].

Although the goal of the LoRa physical-layer design is to provide wide coverage, the single-hop star topology of the current LoRa networks is not the optimal design from the viewpoint of coverage [6]. In such a topology, all the devices communicate directly to a central base station. Therefore, the base stations need to be deployed in particular locations with sufficient density to ensure coverage. Moreover, the single-hop star topology cannot provide satisfactory coverage in some indoor scenarios where the devices are deployed in highly shielded locations such as basements.

Furthermore, the single-hop star topology prevents the LoRa network from utilizing its full capacity. It is well known that LoRa adopts the chirp spread spectrum (CSS) technique. An important parameter in LoRa is the *spreading factor (SF)*. LoRa signals with different SFs are orthogonal to each other [7], and therefore, SFs can be used as an extra dimension for multiple access, thus further increasing the network capacity. However, the throughput rate, receiver sensitivity, and coverage differ vastly between the SFs. Specifically, the lower the SF, the higher is the throughput and the narrower is the coverage. Therefore, with the single-hop star topology, employing SF will allow the areas close to the central base station to utilize high capacity improvement, as illustrated in Fig. 1.

We have been striving to realize an omnipresent and more efficient LoRa network. Firstly, we envision the LoRa network as a multi-hop mesh network where the devices can autonomously relay packets to destinations that cannot be reached via a single hop. Moreover, we also envision that the multi-hop LoRa network can smartly utilize the extra multiple-access dimension provided by different SFs. For example, Fig. 2 (a) shows a multi-hop LoRa network providing higher network coverage by employing multiple relays. Fig. 2 (b) shows the use of clustering for parallel information exchange where a small SF provides higher throughput in local area and large SF allows relaying packets to distant locations. Fig. 2 (c) shows that the SFs can be used to create a pipeline to improve the throughput.

We believe that the concurrent transmission (CT) flooding [8] will be a good candidate for the multi-hop LoRa network. The CT which realizes an ultra-fast back-to-back relaying by introducing synchronized packet collision has been proven to be a more efficient multi-hop protocol. It is essential to verify whether the LoRa receiver can endure co-technology interference (i.e., interference from LoRa packets) to realize a CT-based multi-hop network which exploits the capacity provided by SFs. Especially, in the CT scenario, we need to ensure that the receiver can survive synchronized collisions from LoRa packets using *identical* SF. On the other hand, when SFs are utilized as a dimension for multiplexing, the receiver suffers from an interference with *different* SFs, implying that the orthogonality between the SFs needs to be examined carefully.

In the proposed study, we have extensively evaluated the receiver performance under these two types of interference. The main contributions of this work are as follows.

- We have evaluated LoRa receiver performance in CT

978-1-5386-4790-5/18/$31.00 ©2018 IEEE

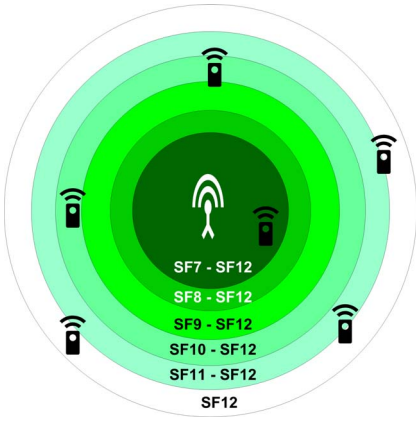

Fig. 1: The coverage of different SFs under singel-hop topology. Only the area near the base station enjoys high capacity.

for different SFs. The simulation results show that larger SFs lead to better performance under interference with identical SFs and identical conditions as compared to smaller SFs. The experiment shows that CT can benefit from the multi-hop LoRa network (CT-LoRa), employing each SF with almost 100 % average packet reception rate (PRR) in practical scenarios.

- We evaluated the receiver performance under co-technology interference using different SFs in both simulation and real-world experiments to verify the orthogonality between different SFs. The results show that the SFs are not fully orthogonal. Although the LoRa recevier has a tolerance of at least -10 dB SIR, the required SIR for successful transmission differs for different SFs. Larger SFs show strong immunity to interference and have less impacts on others, while smaller SFs (especially, the smallest,i.e., SF7 and SF8) are strongly affected by packet collision.
- We conduct a proof-of-concept experiment using SF-pipeline scheduling to assign all SFs to multiple relays. In conventional CT flooding, the next packet is transmitted only after the previous flooding has finished, significantly increasing the flooding duration. The next flooding can be pulled to the end of the 1st-hop relaying by using the structure of the SF-pipeline, as shown in Fig 2,. As compared to CT-LoRa without a pipeline, the flooding duration is reduced by 23.8 % in a six-hop scenario, where each hop uses a different SF. In our real-chip experiment, the average PRR for all SFs is slightly larger than 90 %.

II. LoRa Overview

In this section, we present a brief review of the LoRa modulation and the orthogonality between SFs.

A. The LoRa modulation

Long range (LoRa), is a proprietary LPWAN standard. As evident from public information and the preexisting research [9–12], the essence of LoRa radio modulation format is a combination of CSS and high-order 2^{SF} -ary FSK modulation.

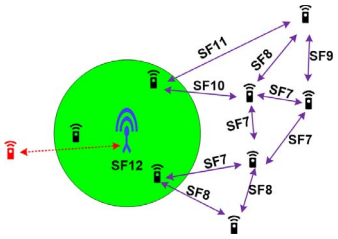

(a) Higher network coverage by using different SFs

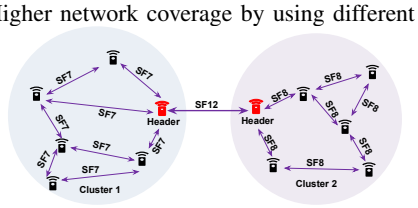

(b) Higher network capacity by using clustering

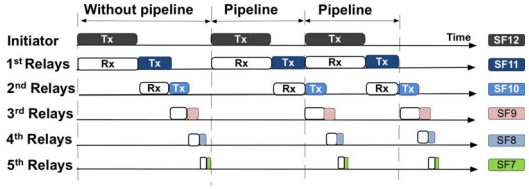

(c) Higher throughput by using pipeline

Fig. 2: Example of coverage extension and more efficient multi-hop LoRa network

More specifically, one LoRa chirp symbol contains 2^{SF} samples and has a symbol length in time of $2^{SF}/BW$, as revealed in LoRa Modulation Basic [7]. The more the samples in one symbol, e.g., 4096 samples with the maximum SF12 and 128 samples with the minimum SF7, yield better sensitivity gain within a fixed bandwidth. Thus, the attractive sensitivity gain is actually provided by a tradeoff of the sampling length.

B. The orthogonality between SFs

Different SFs result in different chirp spreading owing to the CSS. During interference with different SFs, the energy of interference itself will be averaged and the power density will decrease as the interference will spread out over a wide bandwidth. However, the desired signal is still focused in a narrow band after decoding, implying that CSS greatly reduces the effect of different SFs.

III. Receiver Performance under Identical-SF Interference

In this section, we describe the CT-LoRa receiver performance under interference with identical SFs to evaluate whether CT will be effective in the LoRa network for all SFs. First, we present the receiver behaviors created on a simulation platform from SF7 to SF12. Next, we describe several experiments conducted in real environment to support our simulation results.

A. Simulation

In our simulation platform, we generated a one-hop transmitter-channel-receiver channel based on 2^{SF} -ary FSK modulation, further spread by the LoRa chirp signal. The sensitivity gain or loss between two transmitters was determined

to evaluate the LoRa receiver performance under CT. The parameter space and specific setup are listed in the Table I and Table II. Depending on the chosen SF in LoRa network, the *symbol time (T_s)* and the *frequency deviation (f_{dev})* can be calculated in a simple manner using the equation in [7]. Owing to the page limitation for this paper, the full details about simulation are provided in [13].

Para. \ SF	SF12	SF11	SF10	SF9	SF8	SF7
T_s (ms)	32.8	16.4	8.2	4.1	2.05	1.02
f_{dev} (Hz)	30.5	61	122	244	488	976

TABLE I: Parameters for different SFs.

Timing offset (TO)	0 to 4 T_s
Carrier frequency offset (CFO)	0 to 4 f_{dev}
Power offset	0 dB, 1 dB, 2 dB, 3dB
Phase offset	Random (0 to 2π)
Bandwidth	125 KHz
Error correcting code (ECC)	Unused

TABLE II: Simulation setup.

The results for SF7, SF9, SF11, and SF12 are shown in Fig. 3, 4, 5, and 6, respectively. Each subfigure (a), (b), (c), and (d) corresponds to a special power offset (0-3 dB) and the X and Y axes represents CFO and TO, respectively. The sensitivity loss or gain is indicated by a (2-D) contour map where the darkest areas are the areas which are most affected by sensitivity loss. Several observations can be made from these results. They are described in the following subsections.

1) Power effect: In Fig. 3 (a), the surviving zone of SF7 is limited. SF7 CT could barely survive in the LoRa network with zero power offset. When the power offset was increased by 1 dB, the receiver performance improved as per our expectation. Under 2-dB power offset, as shown in Fig. 3 (c), the sensitivity loss was roughly 10 dB lower in SF7, indicating the high potential of application of CT to LoRa network for all SFs in a real environment. Moreover, each figure shows consistent results that the best receptions always appear under the CFO and TO that are half-integers of frequency deviation and symbol time, respectively. The results correspond to our previous analysis based on the maximum SF12 [14].

2) SF difference: Larger SFs yield a clearly better performance under identical conditions as compared with smaller SFs. Even without the power offset, using SF $>$ 9 yields the best performance, with approximately 5 dB sensitivity loss as presented in subplot (a) of each figure. When the power offset exceeds 3 dB, as shown in Fig. 4 (d), 5 (d), 6 (d), the receiver performance is comparable to that in a collision-free case. More specifically, closer SFs present similar results under CT-LoRa, where the smallest value that is SF7 presents the worst results for identical-SF interference, and SF9 and SF11 are similar to each other. The largest of the values, SF12, yields the highest immunity against interference for different SFs.

B. Experiments

We conducted real-chip experiments for all SF in two-building and four-building scenarios in a practical environment to evaluate the efficiency and robustness of CT-LoRa. Specifically, we used 18 LoRa RF modules equipped with Semtech SX1272 and STM32L151 microprocessors to cover the buildings. Each node acts as an initiator in a round-robin manner and the others as relays. In each experiment round, the initiator transmits 100 packets with a 15-byte packet length to trigger CT flooding 100 times for each SF. We show the detailed deployment map in Fig. 7 (a) and (b).

Fig. 8 shows the experiment results under the two scenarios, including the worst and average network PRR and the maximum and average hop count between any two nodes according to each SF. From the experiments, the following observations were made.

1) Immunity against identical-SF interference: As seen in the simulation analysis results, Fig. 8 shows that the larger SF provides stronger immunity against identical-SF interference. In Fig. 8 (a) and (c), all SFs shows an average network PRR exceeding 99 $\%$ for both two scenarios under CT-LoRa. The results show that the performance of CT-LoRa using all SFs is still robust to destructive packet collisions. On the other hand, smaller SFs present worse network PRR as compared to the larger SFs. For SF7, PRR was approximately 80 $\%$ PRR, while for others, it was close to 90 $\%$ in the two-building experiment.

2) Coverage of different SFs: Fig 8 (b) and (d) proves that even LoRa has a notable coverage range under each SF. In the indoor environment where some nodes may be considerably shielded, a multi-hop LoRa network is much more flexible and necessary to guarantee coverage. In our experiment, to cover two buildings, the maximum hop count while using SF12 was three hops and four hops for SF7, as shown in Fig. 8 (b). Moreover, the hop count results for both scenarios show differences in coverage between SFs, corresponding to our previous analysis results. Even the network performance is similar to others; Fig 8 (c) shows a 22 $\%$ and 68 $\%$ worst PRR between two nodes under SF7 and SF8, respectively, when covering four buildings. This result shows that the higher efficiency presented by the smaller SF is obtained by sacrificing the sensitivity of LoRa signal. Additionally, the use of a single SF has limitations and is inefficient to guarantee the robustness of a multi-hop CT-LoRa network.

IV. Receiver Performance under Different SF Interference

In order to verify the orthogonality between different SFs, we evaluated the required minimum SIR at which LoRa still can survive different-SF interference. We first verified the orthogonality between different SFs by using the simulation platform. Additionally, we conducted a series of experiments to verify our simulation observations.

A. Simulation of orthogonality between SFs

In the simulation, we considered the single hop scenario with one transmitter and receiver. The transmitter and receiver

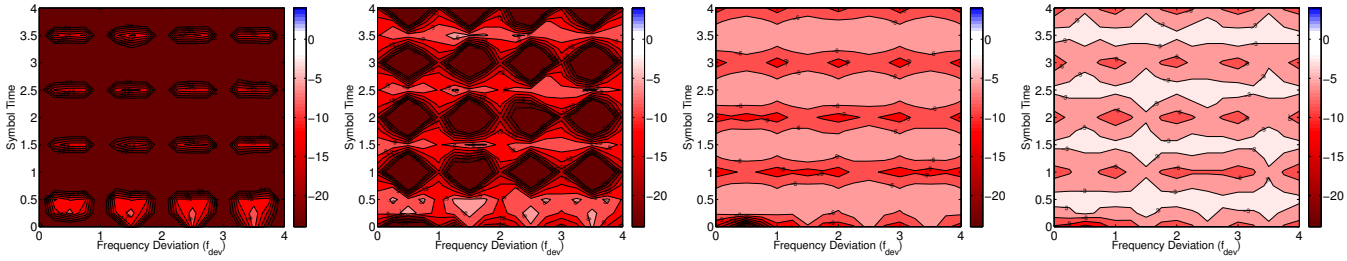

(a) Power offset: 0 dB (b) Power offset: 1 dB (c) Power offset: 2 dB (d) Power offset: 3 dB

Fig. 3: Simulation results for SF7. The X and Y axes represent the CFO (0 - 4 f_{dev}) and timing offset (0 - 4 T_s). The color in the two-dimensional (2-D) contour map indicates the degree of sensitivity loss or gain.

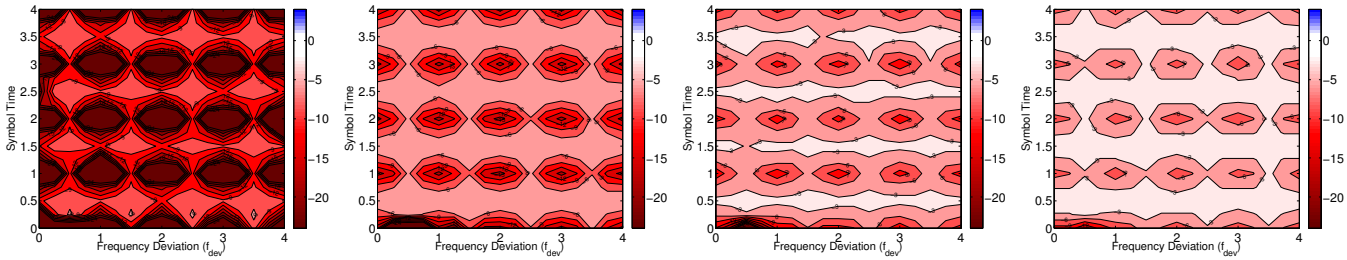

(a) Power offset: 0 dB (b) Power offset: 1 dB (c) Power offset: 2 dB (d) Power offset: 3 dB

Fig. 4: Simulation results of SF9.

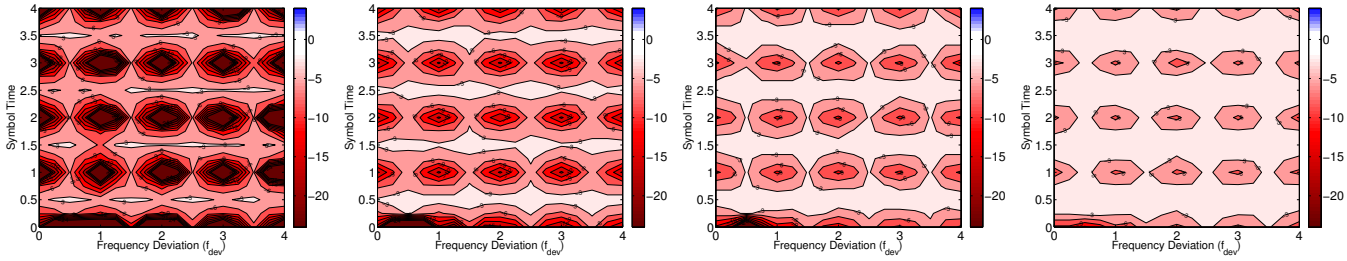

(a) Power offset: 0 dB (b) Power offset: 1 dB (c) Power offset: 2 dB (d) Power offset: 3 dB

Fig. 5: Simulation results for SF11.

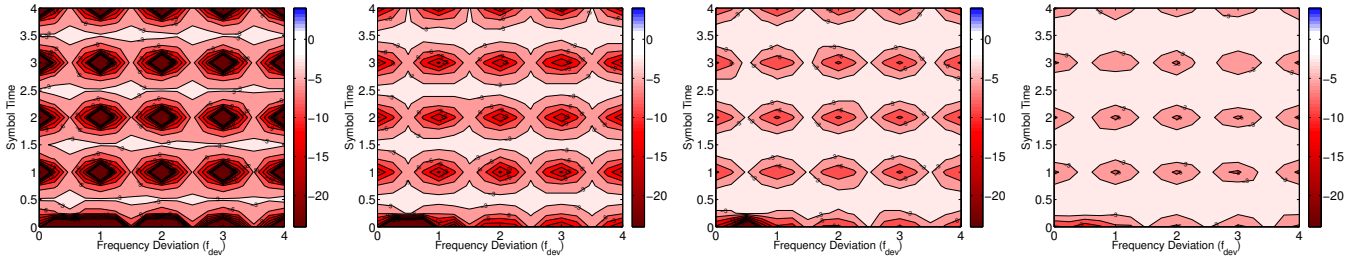

(a) Power offset: 0 dB (b) Power offset: 1 dB (c) Power offset: 2 dB (d) Power offset: 3 dB

Fig. 6: Simulation results for SF12.

with the same SF are referred to as the victim. Another signal with an SF different from the transmitter is considered the interferer. We tested all possible combinations of *victim SF* and *interferer SF*. We also set the wanted signal as 0 dB while changing the power level of the interferer. We recorded the required SIR corresponding to 10 % PRR and 90 % PRR. The thermal noise is set zero.

We present the simulation results in Fig. 9. The figure shows six groups that represent the victim SF on the X-axis, and the colors listed in the legend correspond to different interferer SFs in each group. The Y-axis represents the PRR of each bar between 90 % and 10 %. The case in which the victim and interferer use identical SF is not considered and is not plotted in this figure.

The results show that different SFs provide different tolerances to interference as the SFs are not orthogonal. From the viewpoint of the victim, larger SFs always provide better immunity to interference than the smaller ones. On the X-axis, the results show a clearly decreasing trend as SF increases. In the bar set of SF12, the SIR is roughly -25 dB, while for SF7, it is approximately -12 dB. From the viewpoint of the interferer, in each group, the interference with smaller SF affects the transmission to a greater extent than when using larger SF. As a given example, in the bar set of SF10, with interference with

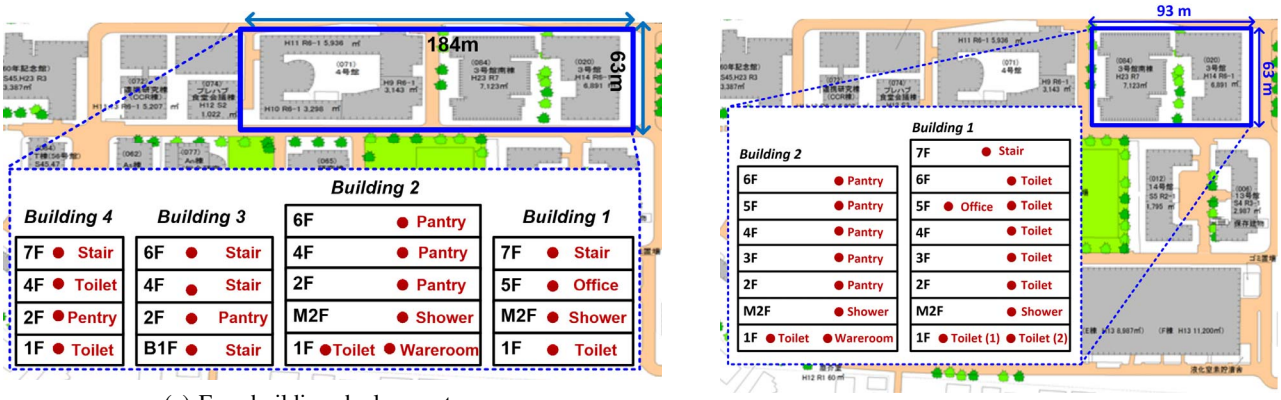

(a) Four-building deployment map

(b) Two-building deployment map

Fig. 7: Experimental deployment of two scenarios.

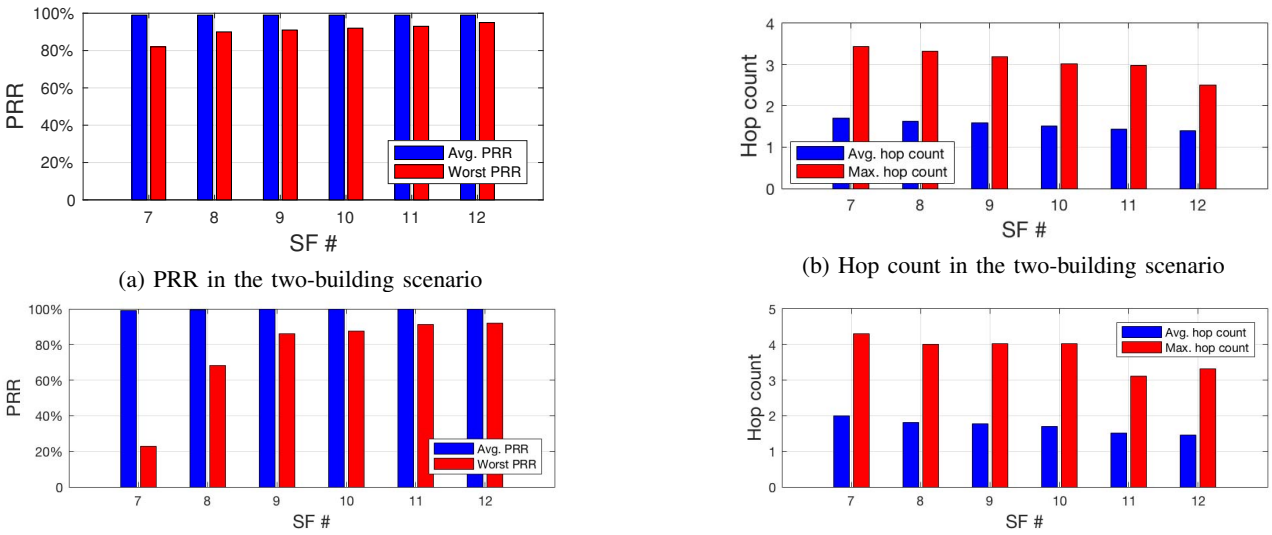

(a) PRR in the two-building scenario

(b) Hop count in the two-building scenario

(c) PRR in the four-building scenario

(d) Hop count in the four-building scenario

Fig. 8: Experimental results for two scenarios.

SF7, the gap of PRR changes from -17 dB to -21 dB, while the value ranges from -23 dB to -24 dB for interference with SF12.

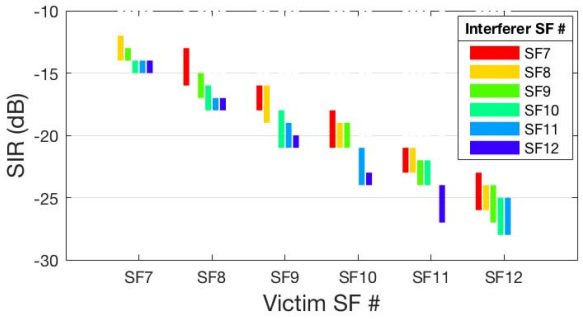

Fig. 9: SIR statistics of each SF with different-SF interference.

B. Experiments of different-SF interference

To further confirm our analysis about the LoRa receiver performance under different-SF interference, we conducted real-chip experiments to determine the required minimum SIR in a real environment.

1) Experiment setup and procedure: We used the three LoRa modules described in Sec. III. The experimental setup is shown in Fig. 10. The interferer broadcasted continuously and uninterruptedly with a specified SF to occupy the whole frequency band during the experiment period. The transmitter sent 100 packets using different SFs in one experiment period, while the receiver recorded the number of packets received successfully. The parameter settings for the experiment were identical to the ones for the simulation, unless specifically mentioned. Note that with the interference with an identical SF, the transmission always fails and dies. During the experiment, the initiator used all SFs, except the same one, for interference.

Initially, we set the transmitter and the receiver at two fixed positions at a distance of 1 m from each other to determine the receiver performance under different SIRs, as shown in Fig. 10. By adjusting the location of the interferer manually within the area between the transceiver and receiver, we recorded the *Received Signal Strength Indication (RSSI)* corresponding to the transmitter and the interferer in the view of the receiver. Finally, we determined the boundary value of

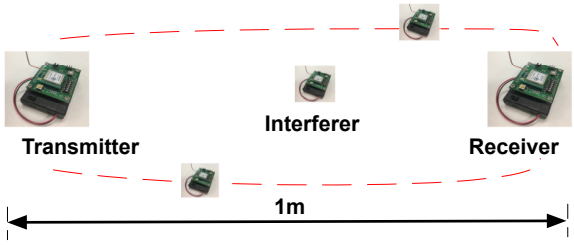

Fig. 10: Interference experiment setup.

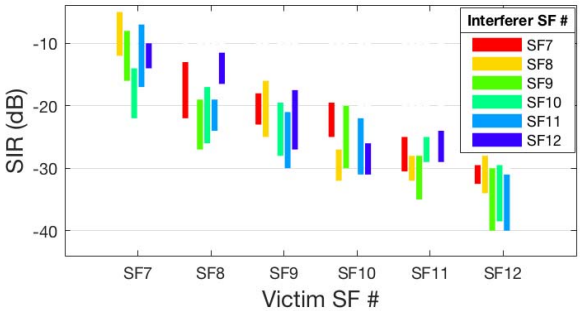

Fig. 11: Experiment results of different-SF interference.

average RSSI when PRR was slightly larger than 90 % or less than 10 %.

2) Results and discussions: The experimental are shown in Fig. 11. The trend is the same as that observed in the simulation analysis. Larger SFs always yielded better performance than smaller ones for different SF interference. We have no knowledge of the LoRa module and the kind of error correcting code (ECC) chosen for LoRa decoding; we expect that the ECC might improve the receiver performance in our real-chip experiment. Specifically, the SIR values in each bar set present approximately 5-dB gain as compared to the simulation results. Furthermore, in the bar set of SF12, SIR ranges from -30 dB to -40 dB and the average SIR of bar SF7 is approximately -15 dB.

Precise control of RSSI and measurement of SIR are difficult in the practical environment. In Fig. 11, each bar set does not show a clear trend for different SF interference. In agreement with the simulation analysis results, the experiment results also present that the smaller SFs are much more sensitive to mutual SF interference.

To further evaluate the orthogonality between SFs, we considered two extreme experimental cases based on the setup environment. The results are shown in Table III and Table IV. In the first case, the interferer is set close to the transmitter deliberately, providing a high SIR from the viewpoint of the receiver. Table III shows that the PRR when using each SF is almost 100 % with a high SIR. However, in some cases, for instance, when the transmission uses SF11 and is under interference from SF8, SF9, and SF10, packet loss occurs because of the possibility that interfering signals collide with the packets.

In another case, the interferer is set close to the receiver to ensure the power of the interfering signal is larger than that of the data packet. As shown in Tab. IV, when the SF value of interference exceeds eight, transmission using all SFs have good performance, achieving almost 100 % PRR. However, when the transmission uses the smallest SF7 and SF8 (shown in the first two columns) and the interference arises from SF7 to SF11, the network almost crashes with a PRR less than 10 %. On the other hand, when interferer uses SF12, the PRR becomes 55 % and 100 %, respectively, clarifying that larger SFs provide better receiver performance. Additionally, when the transmission is subjected to identical-SF interference, the results are not applicable (N/A) in both two tables.

PRR(%) Rev. \ Inf.	SF7	SF8	SF9	SF10	SF11	SF12
SF7	N/A	98	100	100	100	100
SF8	100	N/A	100	100	100	100
SF9	100	97	N/A	100	100	100
SF10	100	100	100	N/A	100	100
SF11	100	98	98	98	N/A	100
SF12	100	100	100	100	100	N/A

TABLE III: Experiment results in high SIR scenario.

PRR(%) Rev. \ Inf.	SF7	SF8	SF9	SF10	SF11	SF12
SF7	N/A	0	99	99	99	99
SF8	0	N/A	100	100	100	100
SF9	<10	<10	N/A	100	100	100
SF10	<10	<10	100	N/A	100	100
SF11	<10	<10	99	100	N/A	100
SF12	55	100	100	100	100	N/A

TABLE IV: Experiment results in low SIR scenario.

V. Combination of SF-pipeline and CT in LoRa Network

Conventionally, next packet transmission in CT is only allowed after the previous flooding is finished. We performed a proof-of-concept experiment combining the CT and SF-pipeline scheduling using different SFs. The SF-pipeline allows the initiator to conduct fast packet transmission, wherein the next flooding is pulled at the end of the 1st-hop relaying. Thus, the transmission in different hops can be overlapped, and therefore, we can enhance the capacity of the LoRa network.

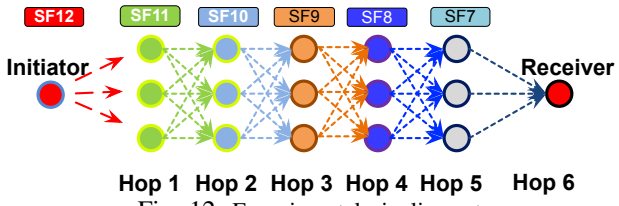

Fig. 12: Experimental pipeline setup.

A. Experiment deployment and procedure

To build the pipeline structure, as shown in Fig. 12, we used all six SFs to multiple relays, where each hop relay uses one SF. The initiator used SF12 in the first hop, while the receiver used SF7 to receive packets from the last hop, and the others relay nodes used different SFs assigned in

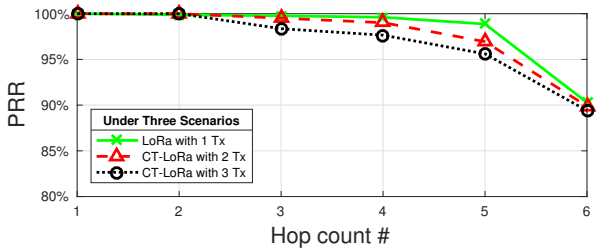

Fig. 13: Network average PRR Using SF-pipeline.

a descending order corresponding to each assigned hop. In this experiment, we evaluated three scenarios according to the number of transmitters in one hop: (1) *LoRa with 1-Tx*, where only one node joins in the transmission and CT does not occur, (2) *CT-LoRa with 2-Tx*, where two nodes participate in CT, and (3) *CT-LoRa with 3-Tx*, where all three nodes join in the transmission. To increase the conflict probability intentionally, we used 17 nodes in a small office room ($13.7 \times 3.7\ m^2$).

The time scheduling of the pipeline is shown in Fig. 2 (c) where the initiator only needs to ensure that the first set of relays could receive the next packet just after the last one was delivered. In the experiment, the interval of broadcasting could be equal to the packet length of SF11. The initiator broadcasted 1000 packets each time, and all the relays using different SFs were set against the interference from SF12 except the first relays and vice versa. In one pipeline cycle, we could easily compute that the flooding duration decreased by 23.8 % with five hop relays.

B. Results and discussions

The results of SF-pipelining under three different scenarios are shown in Fig. 12. On the X-axis, the hop count corresponds to SF12-SF7, while the Y-axis shows the average PRR in each case.

By exploiting the SF-pipeline to enable fast flooding in CT-LoRa, the network remains robust and efficient, preventing any significant performance degradation. The CT-LoRa network shows a good network performance, with the PRR maintained roughly at 90 %. More specifically, the largest SF12 still shows a 100 % PRR under interference from SF11 to SF7, in agreement with our analysis results described in the previous sections. Even SF11 is not affected by interference from others, and both with/without CT cases present consistent results of almost 100 % PRR. The performance when using smaller SFs starts degrading owing to the different immunity against interference. Moreover, the worst case is seen when using SF7, which shows a PRR of roughly 90 %. However, in real environment, the network performance of CT-LoRa with a pipeline is still comparable to that of the pipeline without CT. The results show the efficiency of using smaller SF and the higher immunity against mutual SF interference when using the larger SFs.

VI. Conclusion and Future Work

The LoRa standard provides wide coverage and great flexibility between sensitivity and throughput by utilizing different SFs. However, the single-hop star topology limits the efficiency and coverage ability, while a multi-hop LoRa network not only optimizes the coverage to support extreme environments but also presents the potential to realize multiple-access by exploiting multiple SFs. To achieve this goal, we verified the LoRa receiver performance under CT with all SFs. With sufficient power offset, CT-LoRa exhibited good performance under packet collision with identical SFs. Performance with smaller SFs was more sensitive to power offset and interference. We evaluated the orthogonality between mutual SFs, owing to which different SIRs are required to transmit the packets successfully using different SFs. Additionally, through a proof-of-concept experiment, we showed the feasibility of fast flooding over multi-hop LoRa network using the SF-pipeline that shortens the flooding duration.

In our future work, the pipeline scheduling and SF would be selected carefully as different SFs do not have symmetrical data rates and immunity against mutual SF interference. Then, SFs based on the network status would be adaptively assigned to achieve the full capacity of the network.

Acknowledgment

This work was supported in part by the Cross-Ministerial Strategic Innovation Promotion Program, "Infrastructure Maintenance, Renewal, and Management Technology" and in part by JSPS Grant-in-Aid for Scientific Research (A) under Grant JP16H02358.

References

[1] S. Zhu and N. Zhang, "A research about return channel of terrestrial digital based LPWAN," in *Proc. IEEE ICCCI '16*, Oct. 2016, pp. 296–299.
[2] J. Petäjäjärvi, K. Mikhaylov, R. Yasmin, and et al., "Evaluation of LoRa LPWAN technology for indoor remote health and wellbeing monitoring," *Int. J. Wireless Inf. Networks*, vol. 24, no. 2, pp. 153–165, 2017.
[3] C. Pham, "QoS for Long-Range wireless sensors under Duty-Cycle regulations with shared activity time usage," *ACM Trans. Sen. Netw.*, vol. 12, no. 4, pp. 33:1–33:31, Sep. 2016.
[4] D. H. Kim, J. B. Park, J. H. Shin, and J. D. Kim, "Design and implementation of object tracking system based on LoRa," in *Proc. ICOIN '17*, Jan. 2017, pp. 463–467.
[5] "Lora Alliance," http://www.lora-alliance.org/.
[6] K. H. Ke, Q. W. Liang, G. J. Zeng, J. H. Lin, and H. C. Lee, "A LoRa wireless mesh networking module for campus-scale monitoring: Demo abstract," in *Proc. ACM/IEEE IPSN '17*, 2017, pp. 259–260.
[7] SEMTECH, "LoRa™ modulation basics," Apr. 2016.
[8] F. Ferrari *et al.*, "Efficient network flooding and time synchronization with Glossy," in *Proc. ACM/IEEE IPSN '11*, Apr. 2011, pp. 73 –84.
[9] M. Knight and B. Seeber, "Decoding LoRa: Realizing a modern LPWAN with SDR," *GRCon*, vol. 1, no. 1, Sep. 2016.
[10] T. Petrić, M. Goessens, L. Nuaymi, L. Toutain, and A. Pelov, "Measurements, performance and analysis of LoRa FABIAN, a real-world implementation of LPWAN," in *Proc. IEEE PIMRC '16*, Sep. 2016, pp. 1–7.
[11] E. Ruano Lin, *LoRa protocol. Evaluations, Limitations and Practical test*. Universitat Politècnica de Catalunya, May 2016.
[12] K. Mikhaylov, J. Petäjäjärvi, and T. Haenninen, "Analysis of capacity and scalability of the LoRa low power wide area network technology," in *Proc. EW '16*, May 2016, pp. 1–6.
[13] C. H. Liao, Y. Katsumata, M.Suzuki, and H. Morikawa, "Revisiting the So-Called constructive interference in concurrent transmission," in *Proc. IEEE LCN '16*, Nov. 2016, pp. 280–288.
[14] C. H. Liao, G. Zhu, D. Kuwabara, M. Suzuki, and H. Morikawa, "Multi-hop lora networks enabled by concurrent transmission," *IEEE Access*, vol. 5, pp. 21 430–21 446, 2017.